Journal of The Electrochemical Society, **151** (4) C262-C271 (2004)
0013-4651/2004/151(4)/C262/10/$7.00 © The Electrochemical Society, Inc.

Electrodeposition of Copper in the SPS-PEG-Cl Additive System

I. Kinetic Measurements: Influence of SPS

T. P. Moffat,*,z D. Wheeler, and D. Josell

National Institute of Standards and Technology, Gaithersburg, Maryland 20899, USA

The kinetics of copper electrodeposition from an acidified cupric sulfate electrolyte containing SPS-PEG-Cl were examined. Voltammetric and chronoamperometric experiments reveal a competition between poly(ethylene glycol) (PEG) and $Na_2[SO_3(CH_2)_3S]_2$ (SPS) for surface sites. PEG interacts synergistically with Cl^- and Cu^+ to form a passivating film that inhibits the metal deposition rate by two orders of magnitude. Subsequent adsorption of short chain disulfide or thiol molecules with a sulfonate-end group(s) leads to the disruption and/or displacement of the passivating surface complex and acceleration of the metal deposition rate. The effect of submonolayer quantities of catalytic SPS is sustained even after extensive metal deposition, indicating that the catalyst largely remains segregated on the growth surface. Multicycle voltammetry reveals a significant potential dependence for SPS adsorption as well as its subsequent deactivation. Catalyst deactivation, or consumption, was examined by monitoring the quenching of the metal deposition rate occurring on SPS-derivatized electrodes in a SPS-free electrolyte. Catalyst consumption is a higher order process in terms of its coverage dependence and a maximum deactivation rate is observed near an overpotential of −0.1 V. Derivatization experiments are shown to be particularly effective in revealing the influence of molecular functionality in additive electroplating. Specifically, the charged sulfonate end group is shown to be central to effective catalysis.
 [DOI: 10.1149/1.1651530]

Manuscript submitted June 11, 2003; revised manuscript received October 16, 2003. Available electronically March 4, 2004.

In the last three years, a curvature-enhanced accelerator coverage (CEAC) mechanism has been shown to quantitatively describe superconformal film growth which is responsible for ''bottom-up superfilling'' of submicrometer features in damascene processing.[1-3] The mechanism has also been shown to apply to silver electrodeposition[4] as well as copper chemical vapor deposition.[5] A key characteristic of superfilling electrolytes, disclosed to date, is the competition between inhibitors and accelerators for electrode surface sites. According to the CEAC model, a thiol or disulfide accelerator, or catalyst, displaces an inhibiting halide-cuprous-polyether species from the interface and remains segregated at the surface during metal deposition.[1-3,6,7] A key consequence of these two stipulations is the possibility that local area change associated with metal deposition on a nonplanar surface may give rise to changes in the local catalyst coverage, (*e.g.*, increases on concave sections and decreases on convex segments) and thereby superconformal film growth. This process is particularly important for surface profiles with dimensions in the submicrometer regime and naturally provides an explanation for the beneficial effects induced by certain additives known as ''brighteners.'' [1,6]

In this first of a series of papers, a more complete assessment of the electrochemical response of planar electrodes in copper superfilling electrolytes is presented. A typical electrolyte contains a dilute, *i.e.*, micromolar, concentration of accelerator in the presence of an inhibitor concentration that is usually an order of magnitude greater. This configuration gives rise to hysteretic voltammetric curves, rising chronoamperometric transients, and decreasing chronopotentiometric traces, all of which reflect the competitive adsorption dynamics occurring between the two species. An underdeveloped aspect of this system is a quantitative description of the mass balance of the additives during plating. Of specific interest is the partitioning of the catalyst between segregation to the free surface *vs.* deactivation by either incorporation into the growing deposit or desorption into the electrolyte. Examination of the metal deposition kinetics on catalyst-derivatized electrodes in a catalyst-free electrolyte is shown to be particularly helpful in quantifying the deactivation process. These experiments also provide an avenue for exploring the impact of various additive functional groups on the metal deposition kinetics.

Experimental

The influence of electrolyte additives on the copper deposition reaction was examined using a variety of electroanalytical methods. Two distinct sets of experiments were performed. The first involved examining the effect of progressive catalyst additions on the metal deposition kinetics in a copper plating electrolyte containing poly(ethylene glycol) (PEG) and Cl-. The second scheme focused on studying the kinetics of copper deposition on catalyst-derivatized electrodes in a catalyst-free PEG-Cl^- electrolyte. The latter set of experiments enabled the effect of the catalyst on the metal deposition rate, along with its consumption, to be examined independent of the dynamics associated with the catalyst adsorption step.

The electrochemical measurements were performed at room temperature in a separated cell. The working electrode compartment contained ~900 mL of electrolyte while 50 mL was held in a counter electrode compartment isolated from the main cell by a Nafion 417[a] membrane. The membrane prevented contamination of the working electrode cell by anode products which are known to perturb the metal deposition kinetics.[8] No deaeration was used in the experiments reported herein. The copper plating electrolytes contained 0.25 mol/L $CuSO_4$ and 1.8 mol/L H_2SO_4. The additives were mixed with the base electrolyte at room temperature either by direct addition as salt or through dilution from a stock solution. The base electrolyte used for most of the experiments described in this report contained additions of 1 mmol/L NaCl (Fischer) and 88 μmol/L PEG (3400 Mw; Aldrich), which yield significant inhibition of the copper deposition reaction. The impact of catalyst additions was examined by mixing $Na_2[SO_3(CH_2)_3S]_2$ (SPS; Rasching, Inc.) with the PEG-Cl^- base plating electrolyte. SPS additions were made from a 500 μmol/L stock solution prepared at room temperature using the base PEG-Cl^- electrolyte. Aliquots from the stock solution were transferred to the working electrode compartment using a microliter pipette. This permitted easy control of electrolyte composition into the submicromolar regime.

The electrodes were prepared by polishing oxygen-free high-conductivity (OFHC) copper plate with ~600 grade SiC paper. For halide-free studies polishing was performed using 18 MΩ water. The rolled copper plate had a (100) recrystallization texture. The freshly polished electrodes were masked with 3M plater's tape, leaving an exposed circular area of ~2.62 cm^2. All experiments were

* Electrochemical Society Active Member.
z E-mail: thomas.moffat@nist.gov

[a] Disclaimer: Product names are included only for accuracy of experimental description. They do not imply NIST endorsement.

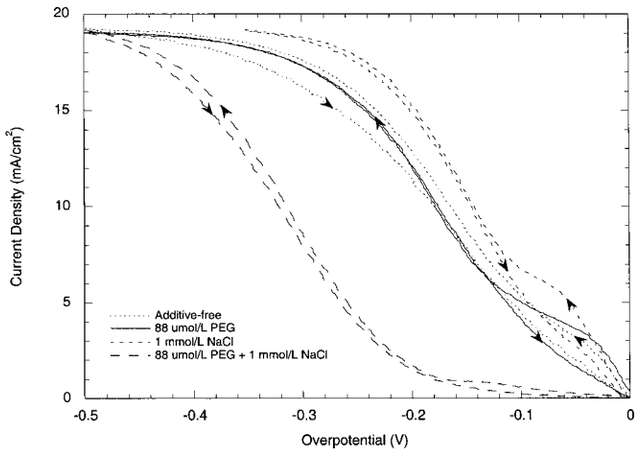

Figure 1. Inhibition of copper deposition from 0.24 mol/L $CuSO_4$ + 1.8 M H_2SO_4 is provided only by the simultaneous addition of Cl^- and PEG. The η-i curves were obtained at 1 mV/s.

initiated under quiescent conditions with free-convection being induced by the Cu^{2+} gradients which accompany metal deposition. A saturated calomel reference electrode (SCE) was used for most experiments, while a copper wire quasi-reference electrode was used for examining the behavior of halide-free electrolytes. The potentials reported in this paper correspond to overpotentials for copper deposition. All voltammetric experiments were performed at 1 mV/s.

In order to examine the rate of catalyst deactivation, or consumption, electrodes were derivatized with SPS or $NaSO_3(CH_2)_3SH$ (MPS; Aldrich) to obtain a given catalyst coverage and then transferred for electroplating in the catalyst-free PEG-Cl^- base electrolyte. Electrode modification was performed by immersion for a controlled period of time in a 1.8 mol/L H_2SO_4 solution containing either 0.5 μmol/L SPS or 1 mmol/L MPS. The electrode was rinsed in water and dried using a tetrafluoroethane duster. Within a few seconds, the derivatized electrode was immersed in the catalyst-free PEG-Cl^- base electrolyte, and copper deposition was monitored under potentiostatic or potentiodynamic conditions.

Electrode derivatization experiments were also used to study the effect of different terminal groups (-CH_3, -OH, -COOH, -SO_3^-) and alkyl chain length (C_2, C_3, C_{16}) on catalyst operation. Derivatization with hydrophobic methyl-terminated thiols, $HS(CH_2)_2CH_3$ (Aldrich), $HS(CH_2)_{15}CH_3$ (Aldrich), and a hydrophilic thiol, $HS(CH_2)_3OH$ (Aldrich), was performed in ethanolic solutions containing 1 mmol/L of the respective molecule. Derivatization with the sulfonate and carboxylic acid-terminated molecules was done in 1.8 M H_2SO_4 containing 1 mmol/L of either SPS, MPS, $NaSO_3(CH_2)_2SH$ (Aldrich), or $HS(CH_2)_2COOH$ (Avocado Research Chemicals, Inc.). The influence of the solvent used for the derivatization was examined by comparing the results for $S(CH_2)_3COOH$-modified electrodes prepared in 1.8 M H_2SO_4 with that obtained from an ethanolic solvent; no significant impact was noted during subsequent metal deposition studies in the PEG-Cl-containing electrolyte. Likewise, exposure of a fresh polished copper electrode to ethanol did not significantly alter the metal deposition behavior.

Results and Discussion

Voltammetry.—Inhibition. Synergistic PEG-halide interaction.—It is well known that the addition of PEG and Cl^- to an additive-free copper plating electrolyte results in strong suppression of the metal deposition rate.[9-15] Significant inhibition occurs only when both components are present in the electrolyte. This is seen in Fig. 1 where the addition of PEG alone exerts a negligible influence on the copper deposition reaction while the addition of Cl^- alone yields a measurable increase in the deposition rate, in agreement with previous reports.[16,17] In contrast, the addition of both PEG and Cl^- together results in clear inhibition of the copper deposition reaction that has been attributed to the formation of a complex layer involving Cl^-, Cu^+, and PEG.[10]

Table I. Kinetics parameters.

$$i = i_o\left(1 - \frac{i}{i_L}\right)\left[\exp\left(\frac{-\alpha F\eta}{RT}\right) - \exp\left(\frac{(1-\alpha)F\eta}{RT}\right)\right]$$

Electrolyte composition	Transfer coefficient α	Exchange current density i_o (mA/cm²)
Additive-free	0.4-0.45	1.4-1.1
PEG	0.45	0.9
Cl	0.5	1.3
PEG-Cl	0.5	0.039
SPS-modified electrode in PEG-Cl	0.5-0.4	4.5-2.25

For copper plating at ~10 mA/cm², *i.e.*, half the limiting current, deposition occurs under mixed control. At higher overpotentials the reaction is diffusion limited with a hydrodynamic boundary layer. The boundary layer is defined by free convection driven by the Cu^{2+} gradient that develops in front of the vertically oriented working electrode. An estimate of the steady-state boundary layer thickness is 99 μm based on the limiting current density of 19.4 mA/cm² and a Cu^{2+} diffusion coefficient of 4×10^{-6} cm²/s.

The overpotential-current density (η-i) curves shown in Fig. 1 can be described by the generalized Butler-Volmer equation using the transfer coefficients, α, and exchange current densities, i_o, shown in Table I. The fitting procedure was biased to accurately describe the behavior for current densities greater than 5 mA/cm²; no attempt was made to describe the peak(s) evident at small overpotentials. This description also does not account for the slightly diminished current on the return sweep, which is visible as minor η-i hysteresis due to some unknown relaxation process. The electrodes visibly roughen after one voltammetric cycle, although this is not reflected in the η-i hysteresis. The shapes of all the curves are reasonably described by a transfer coefficient between 0.4 and 0.5. The combined addition of PEG and Cl^- results in a decrease of the exchange current by almost two orders of magnitude, from ~1.4 mA/cm² to 0.039 mA/cm², relative to the additive-free case. The small variation in the transfer coefficient suggests that the mechanism, or rate-limiting step, of the copper reduction reaction remains largely unaltered by the PEG-Cl^--Cu^+ barrier layer; the blocking layer simply limits access of aquo-cupric ions to the metal surface. A similar conclusion based on impedance measurements was previously reported.[15] However, little information is available concerning the thickness, composition, and/or structure of the passivating film.

The surface active nature of PEG is well known, and significant foaming of the electrolyte is evident if sparged. Thus, immersion of copper into a quiescent PEG-Cl^- plating solution exposes the surface to a high concentration of the polyether species. Simultaneously, the surface is oxidized by Cu^{2+}, yielding unstable Cu^+ which is available to form complexes with Cl^- (and PEG). The combination of these effects suggests that immersion of copper under open-circuit conditions results in a reactive form of Langmuir-Blodgett electrode derivatization.

The effects of variation of the PEG and Cl^- concentration have been studied and will be described in a separate publication. Briefly summarizing, for a PEG concentration of 88 μmol/L, the optimum Cl^- concentration lies between 0.2 and 1 mmol/L. At lower concentrations, Cl^- consumption becomes significant relative to the kinetics of accumulation at the interface; this is manifest as hysteretic η-i behavior.[18] At higher Cl^- concentrations, a decrease in inhibition is observed coincident with the appearance of an additional redox

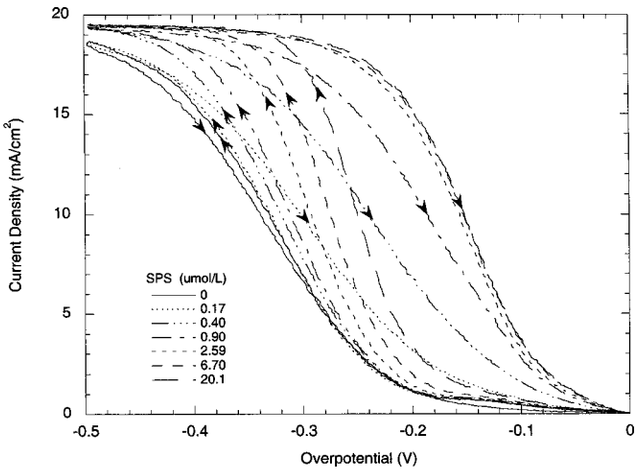

Figure 2. Hysteretic η-i curves are obtained when SPS is added to the inhibiting PEG-Cl electrolyte. The response on the return sweep is effectively saturated beyond 2.59 μmol/L SPS.

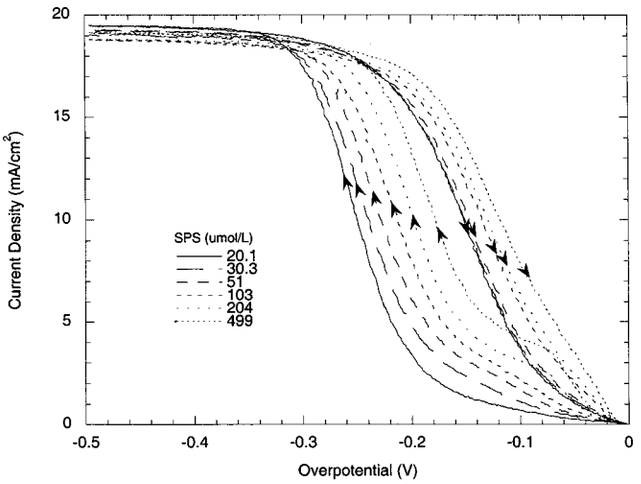

Figure 3. Beyond ~30 μmol/L SPS, an additional wave is evident at −0.1 V. The saturation associated with return sweeps is exceeded when SPS > 50 μmol/L. This is at least partly due to increased surface roughness.

wave and precipitation of CuCl.[16,19] For [PEG] > 8 μM, stable inhibition is apparent for a sweep rate of 1 mV/s and [Cl^-] = 1 mmol/L. Path- and time-dependent hysteretic behavior are evident at lower PEG concentrations. The latter hysteresis is a consequence of potential-dependent disruption of the blocking layer convoluted with transport-limited access of PEG to the surface. In order to minimize or circumvent the effects associated with time-dependent phenomenon linked to PEG-Cl, the 88 μmol/L PEG − 1 mM Cl^- additive combination was used in all the experiments described herein. Deposition in this electrolyte is understood to serve as a reference point characterizing inhibited behavior.

Influence of SPS.—The addition of SPS to the PEG-Cl^- electrolyte results in several notable changes in η-i behavior as shown in Fig. 2. A distinct hysteretic response, where the deposition rate increases substantially during the reverse sweep, is evident for even the most dilute SPS addition shown. This is accompanied by significant brightening of the plated surface; the absence of roughening indicates that the hysteretic behavior must derive from a change in interfacial chemistry rather than surface area. The metal deposition rate at a given potential on the negative-going sweep increases with increasing SPS concentration, and the area enclosed in the hysteretic η-i loop also becomes larger. For the scan rate and switching potential employed here, the hysteresis is maximized for a SPS concentration between 0.9 and 2.59 μmol/L. Further additions of SPS result in progressively higher deposition rates on the negative-going sweep, but the response on the return scan is effectively saturated. The hysteretic response may be understood in terms of disruption of the rapidly formed PEG-Cl^- blocking layer by thiolate or disulfide absorption as suggested previously.[20] SPS-induced depassivation effectively accelerates the metal deposition reaction without requiring any change in the Cu^{2+}/Cu reduction mechanism per se, *i.e.*, catalytic activation of a blocked electrode.

When the SPS concentration exceeds 50 μmol/L, an additional wave is evident on the negative-going sweep as shown in Fig. 3. The wave, at *ca.* −0.09 V, arises from a combination of two distinct processes involving heterogeneous and homogeneous chemistry. First, at such concentrations SPS is no longer dilute relative to the PEG-Cl^- (88 μmol/L to 1 mmol/L) concentration, and SPS competes directly with PEG-Cl for surface sites on a freshly immersed copper electrode. Indeed, at the highest SPS concentrations, the relatively strong thiol/disulfide/chloride copper interactions can be expected to dominate the surface chemistry. Second, significant homogeneous interactions can occur between SPS, Cl, and Cu^+, particularly at low overpotentials where a substantial Cu^+ activity is present, as demonstrated in a number of rotating ring-disk and related experiments.[11,21-24] There is also the suggestion of a surface-bound univalent intermediate based on impedance measurements.[15,25] The equilibrium aquo Cu^+ ion activity (*i.e.*, ignoring complex formation) in the additive-free system is on the order of 0.4 mmol/L,[21-24] which is greater than the combined concentration of the inhibitor and catalyst used in these experiments. However, as the potential is made more negative the equilibrium cuprous activity (and thus the residence time of the reaction intermediate at the electrode interface) declines, and the reaction channel involving homogeneous interactions between the additives and Cu^+ is cut off; this is reflected in the peak observed in the η-i curves. Other possible processes exist as well, such as reaction between SPS-Cu^+-O_2 to yield MPS and related complexes, which prior experiments indicate to be even more catalytic toward metal deposition in the PEG-Cl system.[8]

The significant increase in current density accompanying the return sweep for [SPS] > 100 μmol/L is at least partially associated with an increase in surface roughness which develops during extended polarization in the presence of significant Cu^{2+} depletion. Roughness evolution and its dependence on SPS concentration is discussed in more detail elsewhere.[6]

Multicycle votammetry.—Continued voltammetric cycling in the SPS-PEG-Cl electrolyte (Fig. 4) reveals that the second negative-going sweep does not track the return sweep of the first cycle. This important observation indicates that significant deactivation of the catalyzed surface is occurring. Close inspection of Fig. 4 indicates that the onset of deactivation does not occur until an overpotential of *ca.* −0.050 V, where the second negative-going sweep clearly departs from the first return sweep. This indicates that catalyst deactivation or consumption is potential dependent. Several multicycle voltammetric experiments (not shown) indicate that the steady-state η-i response (*e.g.*, Fig. 4) is approached after the second negative-going sweep for all SPS concentrations greater than 2.5 μmol/L. Not surprisingly, this concentration threshold also corresponds to the minimum value for which saturation of the hysteretic return sweep alone is reached on the first cycle. Strictly speaking, the precise number of cycles required to reach ''steady state'' also depends on other parameters including the switching potential and scan rate. For significantly higher SPS concentrations (*i.e.*, >50 μmol/L), wider potential range windows, and/or extended scanning, the voltammo-

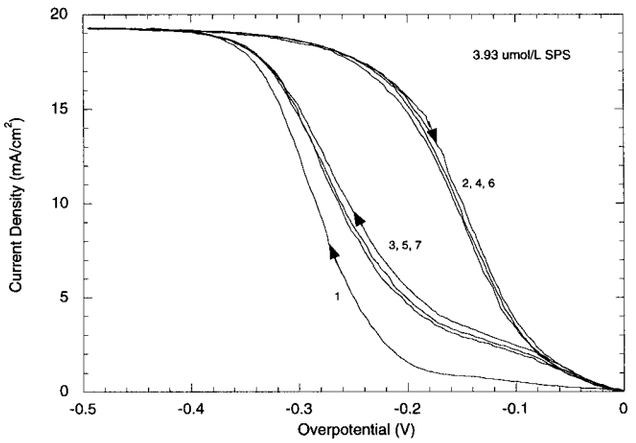

Figure 4. Multicycle voltammetry in the SPS-PEG-Cl system reflects the convolution of potential-dependent SPS adsorption and deactivation. The onset of significant deactivation is clearly evident at −0.08 V. For [SPS] > 2.5 μmol/L a steady-state response is reached after one cycle. The inset numbers reflect the scan sequence.

grams drift due in part to increases in roughness associated with significant deposition under diffusion-limited and mixed-controlled conditions.

Multicycle voltammetry also reveals the influence of potential on the kinetics of catalyst adsorption. A series of voltammograms was collected for different switching overpotentials, E_λ; the sweep rate (1 mV/s) and total scan time (2400 s) were held constant. As shown in Fig. 5a (top) it is clear that the high metal deposition rates that characterize the return sweep for $E_\lambda = -0.45$ V are not accessible for switching overpotentials just 0.2 V lower (*i.e.*, −0.25 V). Voltammograms for two intermediate switching potentials, shown in Fig. 5b (bottom) are consistent with this trend. These results demonstrate that the kinetics of displacement of the inhibiting PEG-Cu^+-Cl^- layer by SPS/MPS adsorption are an increasing function of overpotential; voltammetric cycling to larger overpotentials permits a larger increase in the catalyst surface coverage which manifests as higher currents on the return sweep.

One consequence of the potential-dependent competition between catalyst accumulation and consumption is that the "true" steady-state η-i curve (*i.e.*, for an infinitely slow sweep rate) must lie somewhere between the return sweep (upper bound) and the $2nd^+$ negative-going sweep (lower bound) observed for finite sweep rates.

Chronoamperometry.—The response of the SPS-PEG-Cl system to potentiostatic polarization was investigated over a range of SPS concentration and applied overpotential. In the absence of SPS, the PEG-Cl current transients, shown in Fig. 6, are characterized by ~30 s decay associated with relaxation of the boundary layer that accompanies copper deposition under mixed control. An additional slow decline in the current density is apparent at low overpotentials. This is ascribed to consolidation of the inhibiting overlayer and is analogous to the subtle relaxation observed in the η-i experiments in Fig. 1.

In contrast, electrolytes containing SPS exhibit rising current transients, as shown in Fig. 7. As with the SPS-free electrolyte an initial period (~30 s) of current decay is required to establish the hydrodynamic boundary layer. The subsequent rise in current eventually reaches a steady state. The time required to attain steady state decreases monotonically with SPS concentration. The current transients correspond, qualitatively, to following a vertical trajectory across the hysteretic η-i curves. However, it is evident that the steady-state chronoamperometric current is a function of SPS concentration. This dependence is distinct from the convergence of the

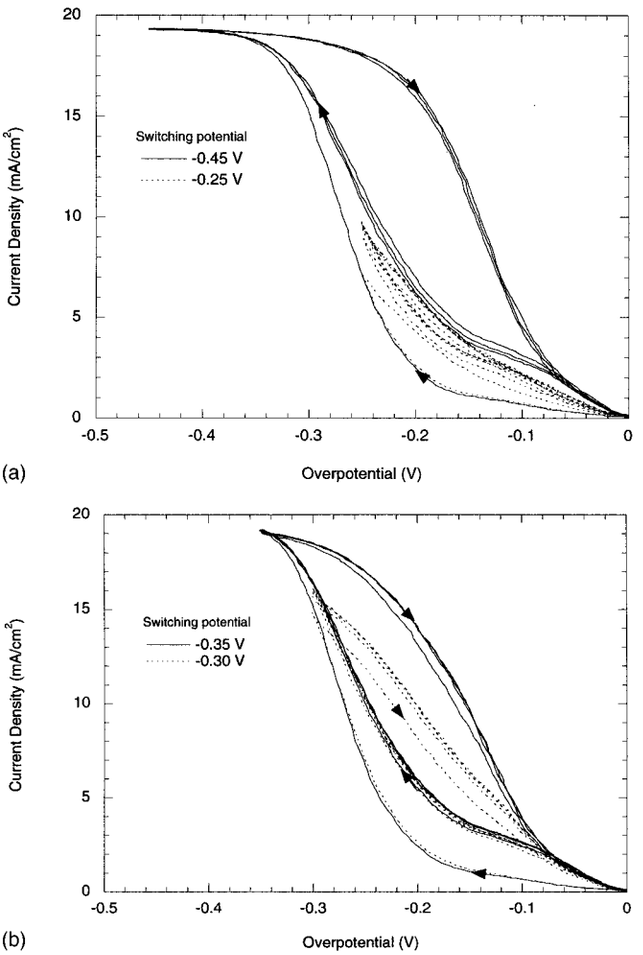

Figure 5. The strong potential dependence of SPS activation is revealed by varying the switching potential, E_λ. A marked increase in hysteresis is evident for $E_\lambda > |-0.25|$ V. The voltammograms were collected for a fixed period of 2400 s. For $E_\lambda = -0.45$ V, an activated state (*e.g.*, $i = 17$ mA/cm^2 at −0.2 V) is obtained on the return sweep after 700 s. In contrast, a maximum current of 5 mA/cm^2 at −0.2 V is observed after 2400 s of cyclic polarization for $E_\lambda = -0.25$ V.

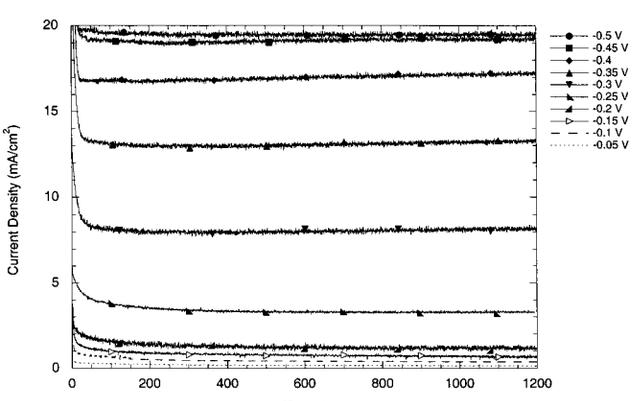

Figure 6. Current transients for copper deposition from the PEG-Cl electrolyte as a function of overpotential. The steady-state currents are congruent with the slow scan, "steady-state" η-i response shown in Fig. 1.

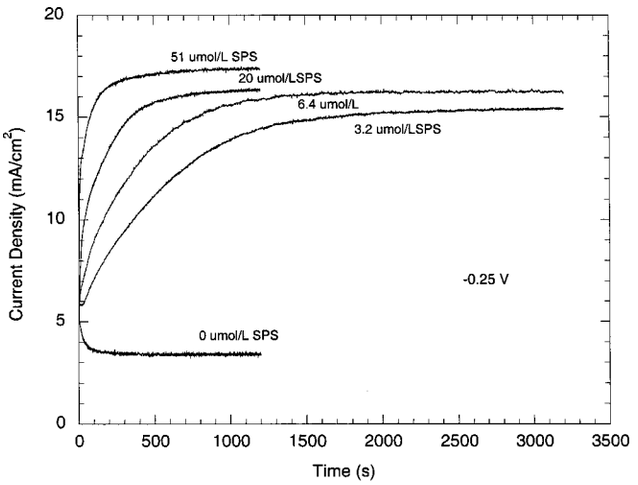

Figure 7. Rising current transients are observed in the SPS-PEG-Cl electrolyte due to activation of PEG-Cl inhibited electrodes induced by SPS adsorption. Qualitatively the transients correspond to following a trajectory across the hysteretic η-i curves shown in Fig. 2. In contrast to the saturated current that characterizes the return sweep of the voltammetric data shown in Fig. 2, the steady-state chronoamperometric current is a function of the SPS concentration.

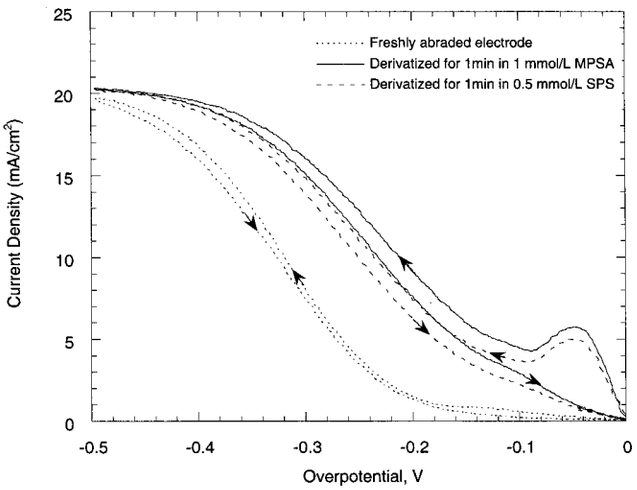

Figure 9. The η-i response for copper deposition on SPS- or MPS-derivatized electrodes in a PEG-Cl electrolyte is compared with that occurring on a freshly abraded surface. The catalytic behavior associated with SPS- and MPS-modified electrodes is ascribed to the sulfonate end-group hindering formation of the blocking PEG-Cl layer.

return sweep η-i data for different SPS concentrations, as shown in Fig. 2. This difference is a result of the potential-dependent catalyst adsorption and consumption which can yield higher catalyst coverages at the higher overpotentials associated with voltammetric cycling. The observed chronoamperometric time constant also decreases with increasing overpotential, as shown in Fig. 8. This is consistent with an increase in the rate of catalyst accumulation at higher overpotentials.

Consumption kinetics.—The preceeding experiments convolve SPS adsorption and consumption; this complicates modeling of the electrical response, making results ambiguous. In order to separate the relative contribution of each process, a series of plating experiments using SPS/MPS-derivatized electrodes in catalyst-free electrolyte were performed; these enable the kinetics of catalyst deactivation, or consumption, to be measured independent of the catalyst adsorption process.

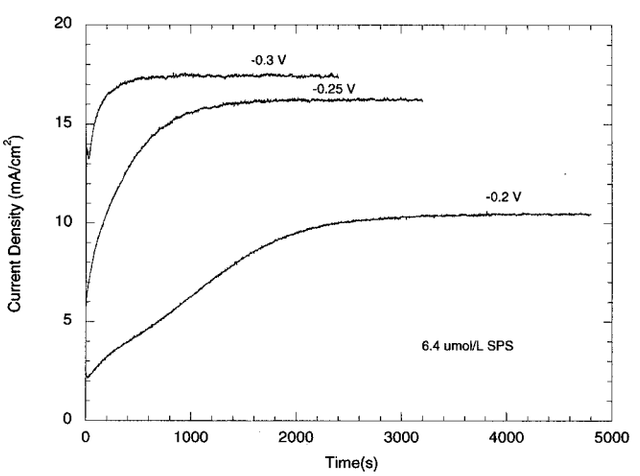

Figure 8. The apparent time constant of the rising chronoamperometric transients increases with overpotential, reflecting the potential dependence for SPS adsorption on PEG-Cl blocked electrodes.

Voltammetry.—The η-i characteristics of electrodes that were derivatized for 60 s in either 1 mmol/L MPS or 0.5 mmol/L SPS are compared in Fig. 9 to the behavior exhibited by a freshly polished electrode during plating in a PEG-Cl^- electrolyte. Derivatization leads to substantial acceleration of the copper deposition rate at low overpotentials. The thiol/disulfide monolayer film clearly prevents formation of the PEG-Cl^- blocking layer under these conditions. The peak at *ca.* −0.05 V reflects the onset of significant catalyst deactivation (discussed earlier). This is followed by the transition to an exponential increase in current while the electrode is subject to a more subtle deactivation process reflected in the decreased current on the return sweep. Approximately five voltammetric cycles are required before the electrode behavior converges with that of a freshly polished electrode. This amounts to passage of ~35 C/cm^2, equivalent to deposition of a ~10 μm thick copper film. Thus, a substantial copper deposit is formed before complete deactivation of the catalyzed electrode occurs.

The onset of significant catalyst consumption at small overpotentials is consistent with that noted earlier for multicycle voltammetry of a freshly polished electrode in the SPS-PEG-Cl electrolyte, *i.e.*, Fig. 5. The peak shape in Fig. 9 suggests that the deactivation process is the dominant process from *ca.* −0.05 V until an inflection is observed at *ca.* −0.09 V, followed by much slower attenuation of the deposition kinetics at higher overpotentials. Multiple voltammetric cycles using a derivatized electrode (not shown) further demonstrates that the most significant decrease in reactivity occurs at small overpotentials. The identity of the precursor, MPS *vs.* SPS, does not affect the results, indicating that the final state of the modified electrode is independent of the differences between the precursors. This is similar to reports that the properties of alkyl monolayer films formed on gold were independent of whether the films were made from thiol or disulfide precursors.[26,27]

A reasonable first estimate of the extent of catalysis provided by a SPS monolayer modified electrode may be determined by fitting the first *ca.* −0.05 V of the η-i curve in Fig. 9 to the Butler-Volmer formalism and assuming negligible deactivation of the catalysts occurs in this range. This yields an exchange current density of *ca.* 4.5-2.25 mA/cm^2, assuming a transfer coefficient of 0.5-0.4. This corresponds to an increase in the deposition rate of ~2 orders of magnitude over that experienced by a freshly polished electrode in the same PEG-Cl electrolyte (see Table I).

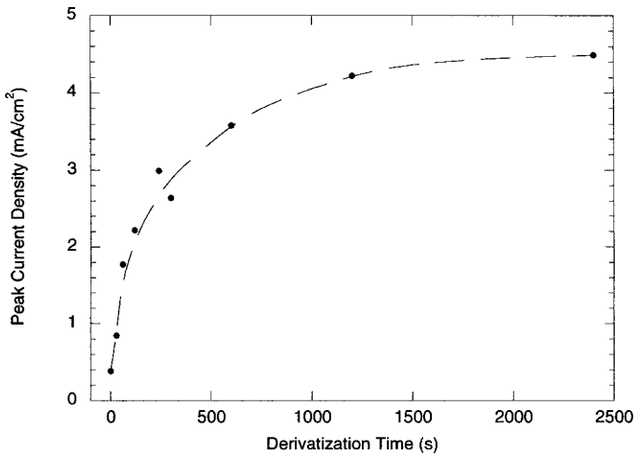

Figure 10. The magnitude of the voltammetric wave at −0.05 V in Fig. 9 is shown as a function of derivatization time. The magnitude of the peak may be used to evaluate the catalyst coverage derived from a given modification treatment.

The magnitude of the voltammetric wave observed at −0.05 V was dependent on the derivatization time and SPS concentration, *i.e.*, the initial catalyst coverage. The maximum or saturation peak current was between 4 and 6 mA/cm^2, depending on the details of the experiment. In a 5 μmol/L SPS solution, saturation of the peak current is observed after >20 min of derivatization (Fig. 10). A similar wave is observed for copper electrodes that are aged under open-circuit conditions in a conventional SPS-PEG-Cl plating electrolyte and can be used for monitoring catalyst accumulation under such circumstances.

Chronamperometry.—The potential dependence of catalyst consumption was examined using samples derivatized for 60 s in either 1 mmol/L MPS or 0.5 mmol/L SPS followed by copper plating in a PEG-Cl$^-$ electrolyte (Fig. 11a, top and b, bottom). Transients for the freshly abraded electrodes (*i.e.*, the same as Fig. 6) represent the baseline toward which the modified electrodes evolve as the catalyst is consumed or deactivated. The derivatized electrodes exhibit notable resilience against passivation by PEG-Cl$^-$. Deactivation at −0.05 V (Fig. 11a) occurs with a time constant of ~200 s, while at −0.25 V (Fig. 11b) catalyst consumption occurs at a rate which is at least an order of magnitude slower. Importantly, the low deactivation rate at −0.25 V is congruent with a basic tenet of the CEAC model of superfilling and brightening, namely, a significant quantity of catalyst floats, or remains segregated, on the surface during copper deposition. The relevant time scale for submicrometer feature filling is <100 s during which negligible attenuation of the deposition rate occurs at −0.25 V. In a related fashion, the thick film grown at −0.25 V was bright and specular while the much thinner deposit grown at −0.05 V was visibly rough.

If electrode deactivation is a manifestation of catalyst consumption alone, then integration of the transients allows an upper bound estimate of catalyst incorporation in the film for a given set of processing conditions. Consider 5000 s of growth at −0.25 V which results in a 30 μm thick film *vs.* growth at −0.05 V which yields a film less than 0.5 μm thick. Assume the derivatized electrodes have an initial disulfide coverage of 6.35×10^{-10} mol/cm^2,[28b] and that the catalyst is completely consumed after 5000 s of electrolysis

[b] Based on literature reports of defected c(2 × 2) and c(2 × 6) structures of short alkane thiols on Cu(100) in vacuum (Ref. 28a and b). Saturation fractional surface coverage of a derivatized electrode estimated to be 0.5 for MPS and 0.25 for SPS based on Cu(100) = 2.55×10^{-9} mol/cm^2, 0.5 coverage = 1.27×10^{-9} mol cm^2, and 0.25 = 6.37×10^{-10} mol/cm^2. Recent work (Ref. 28c) suggests that alkane thiols with bulkier or charged end-groups may exhibit less well-ordered and lower density structures. Thus, these numbers should be treated as an upper bound.

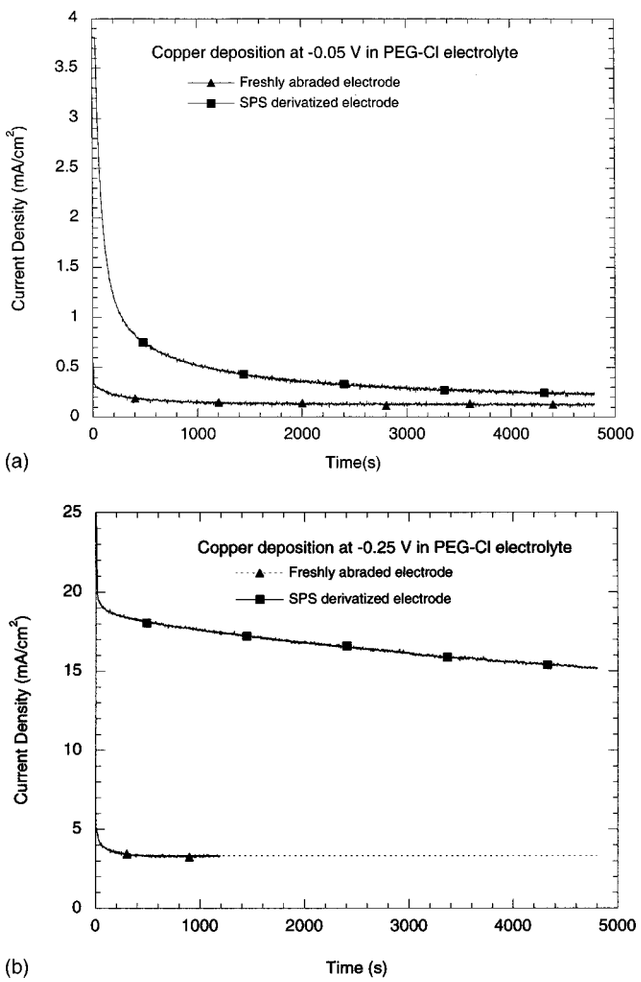

Figure 11. Chronoamperometry reveals the catalytic effect of SPS derivatization. (a) At smaller overpotentials the derivatized electrode is subject to rapid deactivation. (b) In contrast, at higher overpotentials that correspond to practical plating conditions the catalytic effect is sustained for thousands of seconds.

(which is clearly not the case, particularly for higher overpotentials, Fig. 11b). This yields an upper bound of <1 ppm SPS (4 ppm S) incorporated during growth at −0.25 V compared to ~50 ppm SPS (200 ppm S) for deposition at −0.05 V. The calculated impurity level and its dependence on potential compare favorably to published secondary ion mass spectroscopy (SIMS) analysis of copper deposits grown from related industrial electrolytes;[29-31] the O, S, C, and Cl concentration levels are reported to decrease from ~100 to ~1 ppm as the metal deposition rate, *i.e.*, current density, increased.[30] Similar potential-dependent behavior, as well as a significant dependence on hydrodynamics, was reported for another copper plating system.[31] If the entire SPS molecule is incorporated, the C/O/S ratio would be 3/3/2, which compares favorably with SIMS data.[29-31]

The deactivation process was studied over a wide range of potential as shown in Fig. 12. These experiments were repeated on three different occasions and notable dispersion of the time constants was observed; the trends shown in Fig. 12 remain unaltered.[32] The dispersion is most likely due to variations in the derivatization process that may be associated with halide ''contamination.'' This possibility is further complicated by the dynamics associated with chloride coadsorption accompanying subsequent plating in the PEG-Cl electrolyte. It may well be that the catalyst consumption

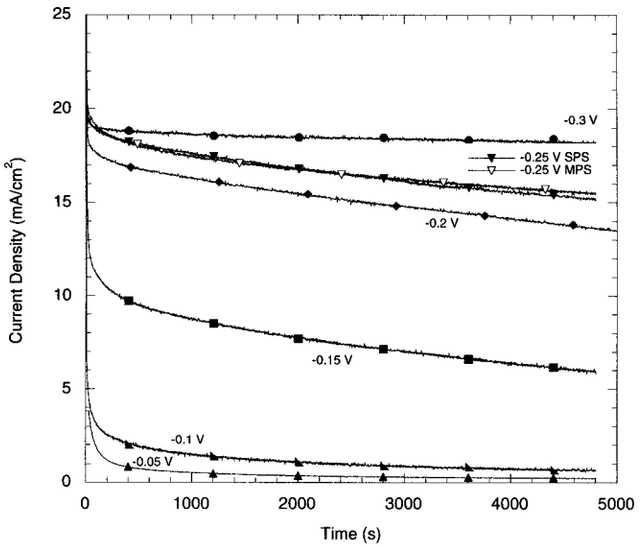

Figure 12. Chronoamperometry detailing the potential dependence of copper deposition on derivatized electrodes. The catalytic effect of derivatization and its strong dependence on potential is readily evident by comparison to Fig. 6. No discernable difference between modification with SPS *vs.* MPS is apparent.

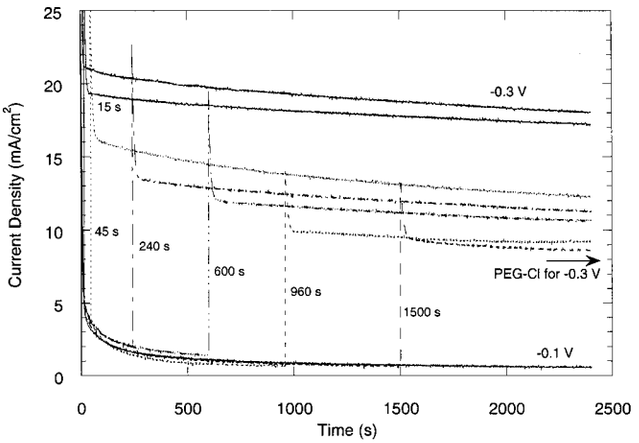

Figure 13. The potential dependence of catalyst consumption is revealed by potential-step experiments during copper deposition in the PEG-Cl electrolyte. Copper was deposited on MPS-modified electrodes for variable times at −0.1 V. This was followed by stepping back to −0.3 V to measure the extent of deactivation. The transients reveal a monotonic decrease in reactivity with time spent at −0.1 V. Catalytic behavior is effectively quenched after 1000 s at −0.1 V. For reference the potentiostatic transients for growth at −0.1 V (rapid deactivation) and −0.3 V (slow deactivation) are shown along with an arrow denoting the steady-state current density for an unactivated (*i.e.*, polished) electrode at −0.3 V in the PEG-Cl electrolyte.

process is hindered by coadsorbed chloride. Other authors have observed irreproducibility in similar modification processes used for studying Cu underpotential deposition (UPD) on modified gold substrates.[33] Nonetheless, comparison of results from derivatized and underivatized electrodes (Fig. 6, 11, and 12) unambiguously reveals that convergence of the respective transients occurs more rapidly at smaller overpotentials, reflecting the enhanced catalyst consumption under these conditions. Quantitative analysis of the transients indicates that consumption is higher order than linear in the catalyst coverage, suggesting the importance of nearest neighbor interactions.[32] No significant dependence on the catalyst precursor identity (SPS *vs.* MPS) was observed, as shown for deposition at −0.25 V.

The potential dependence of catalyst consumption is also readily observed in potential pulse experiments. The potential of a derivatized electrode was first set to −0.3 V, followed by stepping to −0.1 V for a period of time, after which it was returned to −0.3 V. The polarization time at −0.1 V varied between 15 and 1500 s, as shown in Fig. 13. The difference between the current observed at −0.3 V after potential pulsing *vs.* that for unperturbed deposition at −0.3 V clearly reveals that more rapid consumption of the catalyst occurs at lower overpotentials. After polarization at −0.1 V for more than ~1000 s the subsequent electrode response at −0.3 V approaches that of a catalyst-free or deactivated electrode. The increase in consumption with decreasing overpotential indicated by Fig. 13 is consistent with the conclusions derived from Fig. 11.

A variant of the pulse experiment involves studying the effect of aging a derivatized electrode under open-circuit conditions. The similarity of all the deposition transients (Fig. 14) during the first few hundred seconds shows that idling at the rest potential in a PEG-Cl$^-$ electrolyte for 600 s prior to deposition at −0.3 V induces negligible deactivation of the modified electrode. Likewise, deposition at −0.3 V for 600 s followed by a 600 s open-circuit interruption results in negligible attenuation of the rate during subsequent deposition at −0.3 V. Thus, aging under open-circuit condition results in negligible consumption. In contrast, there is a marked deactivation observed at −0.3 V after 600 s of deposition at −0.1 V. This finding demonstrates that the potential-dependent consumption rate exhibits a maximum at intermediate overpotentials, in agreement with the more qualitative conclusion drawn from voltammetric analysis (*i.e.*, Fig. 9).

The ability of a submonolayer quantity of an adsorbed surfactant to impact the film growth processes is well known across a range of deposition technologies. For example, an interesting study of the leveling effect of thiourea on copper deposition ascribes stable growth to a small coverage of deposition rate, suppressing thiourea molecules operating in a gas-like surface state.[34] This adsorbed state is similar to that envisioned here, although in the present case the

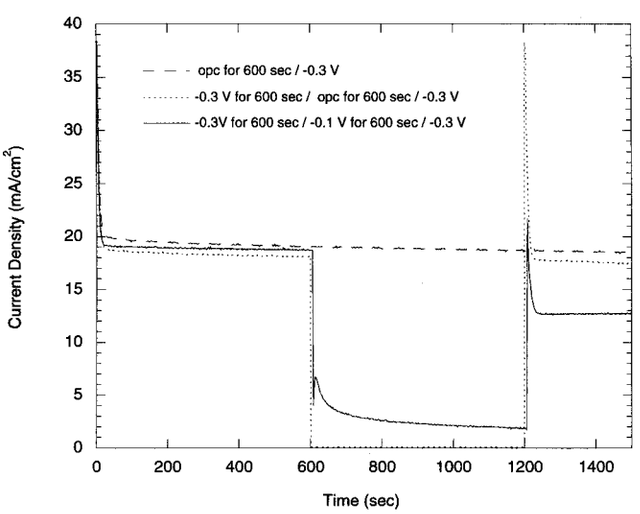

Figure 14. Results of potential-step experiments using an MPS-derivatized electrode. Aging of the derivatized electrode at the open-circuit potential results in negligible deactivation, as evident by the subsequent catalyzed growth at −0.3 V. Likewise, when deposition at −0.3 V is interrupted for aging at open-circuit condition, minimal deactivation is noted during subsequent deposition at −0.3 V. In contrast, significant deactivation of the electrode (as measured at −0.3 V) is evident after metal deposition at −0.1 V. Thus, the potential dependence of catalyst deactivation, or consumption, passes through a maximum at intermediate overpotentials.

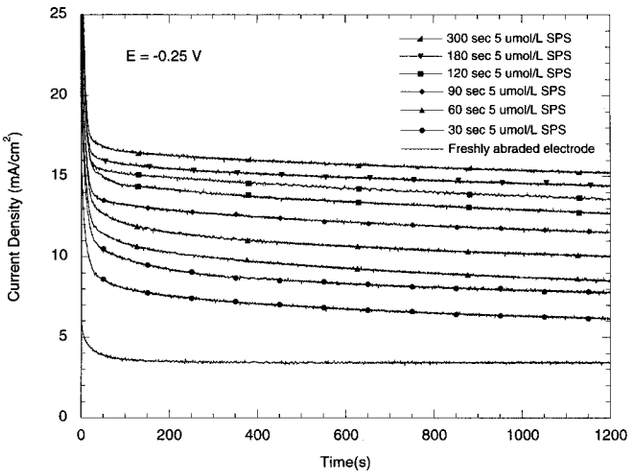

Figure 15. The influence of catalyst coverage on the copper deposition rate at −0.25 V in the PEG-Cl electrolyte. Initial coverage was varied by controlling the derivatization time.

activated species exerts a catalytic influence on the deposition rate. The extent of catalysis provided by submonolayer coverage, along with the associated deactivation dynamics, was examined by varying the electrode derivatization time. As shown in Fig. 15, the copper deposition kinetics in a PEG-Cl^- electrolyte increased monotonically with electrode derivatization time in a 5 μmol/L SPS solution. A doubling of the metal deposition rate is accomplished by derivatization for only 30 s in 5 umol/L SPS, which, as suggested by Fig. 10, corresponds to a small fraction of a monolayer coverage. The transients are characterized by a 30-50 s decay due to relaxation of the hydrodynamic boundary layer. A measurable decrease in reactivity is apparent over the next 1200 s. Nevertheless, for deposition at −0.25 V the extent of deactivation is inconsequential on the ~60 s time scale relevant to filling submicrometer features, again reflecting the propensity of the SPS-derived catalyst to remain segregated at the growing interface.

In general terms, the adsorbed catalyst faces the challenge of ''swimming or sinking'' as copper is being deposited on the surface. The observed maxima in catalyst consumption at low overpotentials, which corresponds to lower deposition rates, is perhaps counterintuitive given that the rate of surface segregation must be finite. Indeed, recent models of additive incorporation have postulated that additive incorporation should be proportional to the current density,[35] a result not borne out for SPS consumption under the present circumstance. An inverse dependence between additive incorporation and the metal deposition rate has been reported for nickel plating from electrolytes which contain a dilute concentration of leveling agent.[36] However, in these leveling systems the inverse dependence was simply a consequence of diffusion-limited accumulation of the additive at the interface during metal deposition. In contrast, the experiments outlined above provide a direct measure of the rate constant of incorporation independent of any limitations associated with the adsorption step.

Catalyst function.—The effect of dialkyl- and diaryl-disulfide additions on copper plating from a simple acidified cupric sulfate electrolyte has been previously examined.[37,38] Anionic sulfonate-terminated molecules were generally found to slightly perturb the copper deposition rate, while diaryl- additions with cationic amino groups resulted in significant inhibition of the metal deposition reaction. In the present work, electrode modification is used to study the behavior of the disulfide and thiol-based catalyst during copper deposition in the presence of PEG-Cl. As with the deactivation experiments, catalyst derivatization allows the complications associated with adsorption from the electrolyte to be avoided and thus represents a powerful method for interrogating the mechanism by which the catalyst functions. Modification with a variety of alternative thiol compounds was used to examine the influence of different terminal groups (-CH_3, -OH, -COOH, -SO_3^-) and alkyl chain lengths (C_2,C_3,C_{16}) on catalytic behavior. The various end groups exhibit different qualities ranging from hydrophobic -CH_3, to hydrophilic -OH, charged -SO_3^-, and reactive -COOH which complexes $Cu^{2+/1+}$.[39] Voltammetry and chronoamperometry were used to evaluate the efficacy of the different terminal groups for preventing the formation of the inhibiting PEG-Cl^--Cu^+ film.

Voltammetry.—After derivatization for 60 s in 1 mmol/L solution of the respective thiols (or 0.5 mmol/L for SPS), the electrodes were dried and transferred to the PEG-Cl^- electrolyte for copper deposition. As shown in Fig. 9 and 16a-c, only electrodes modified with thiols (or disulfide) bearing the -SO_3^- end group exhibit catalytic behavior relative to a freshly abraded electrode. Differences attributable to the disulfide *vs.* thiol head group or variations in the alkyl chain length from C_2 to C_3 represent a minor perturbations relative to the effects induced by the charged -SO_3^- terminal group.

In contrast to the catalytic behavior of -SO_3^--terminated molecules, modification with -$S(CH_2)_2CH_3$ results in a substantial increase in inhibition of the copper deposition reaction, well beyond that associated with formation of the blocking PEG-Cl^- layer (Fig. 16a). Only a very small current is passed until −0.42 V, at which point fresh copper nucleates on top of the monolayer. Once this layer coalesces and the underlying monolayer film is buried, the electrode reverts to the behavior exhibited by a freshly abraded electrode. The -$S(CH_2)_3OH$ and -$S(CH_2)_{15}CH_3$ (Fig. 16b) and -$S(CH_2)_2COOH$ (Fig. 16c) derivatized electrodes also exhibit increased inhibition, although much weaker than that provided by -$S(CH_2)_2CH_3$. Likewise, copper deposition on -$S(CH_2)_2COOH$ and -$S(CH_2)_{15}CH_3$ modified electrodes converges with that of a freshly abraded electrode after the first negative-going sweep, indicating that the monolayer is consumed, *i.e.*, buried.

The greater blocking of the copper deposition reaction provided by -$S(CH_2)_2CH_3$ (Fig. 16a) as compared to -$S(CH_2)_{15}CH_3$ (Fig. 16b) is of interest. This is ascribed to a higher defect density in the -$S(CH_2)_{15}CH_3$ layer associated with its slower, incomplete ordering during the 1 min derivatization treatment. Similar effects have been reported for Cu UPD on gold where C_2 films provided greater inhibition compared to C_3 or C_5 thiols.[33] The differences observed between the hydrophilic -$S(CH_2)_3OH$ (Fig. 16b) and hydrophobic -$S(CH_2)_2CH_3$ (Fig. 16a) modified electrodes draws attention to possible interactions between the monolayer film and PEG in solution. However, similar experiments (not shown) performed in the absence of PEG reveal the same intrinsic behavior, whereby the hydrophobic film -$S(CH_2)_2CH_3$ alone accounts for the remarkable resistance to metal deposition. Analysis of the -$S(CH_2)_2COOH$ modified electrode response is significantly complicated by the well-known reactivity between the -COOH end group and Cu^+/Cu^{2+}.[39] In any case, the transient inhibition provided by the -CH_3, -COOH, and -OH terminated thiols is in good agreement with prior reports of bulk copper and silver deposition on derivatized gold surfaces.[33,40-42]

Chronoamperometry.—Similar trends are evident during potentiostatic deposition under conditions directly relevant to superfilling experiments. As shown in Fig. 17, only electrodes modified with -SO_3^--terminated thiols (or disulfides) exhibit significant catalytic activity. Interestingly, the longer alkyl chain (C_3) of SPS and MPS exhibits slower deactivation kinetics compared to -$S(CH_2)_2SO_3^-$ (C_2), and thus they are more effective catalysts for damascene processing. As noted before, no discernable difference is observed between electrodes modified with SPS *vs.* MPS. In contrast, derivatization with -$S(CH_2)_3OH$ and -$S(CH_2)_2COOH$ results in a transient increase in inhibition which subsequently decreases, yielding behavior typical of a freshly abraded electrode. This relaxation occurs after the deposition of ~50 nm of copper for the

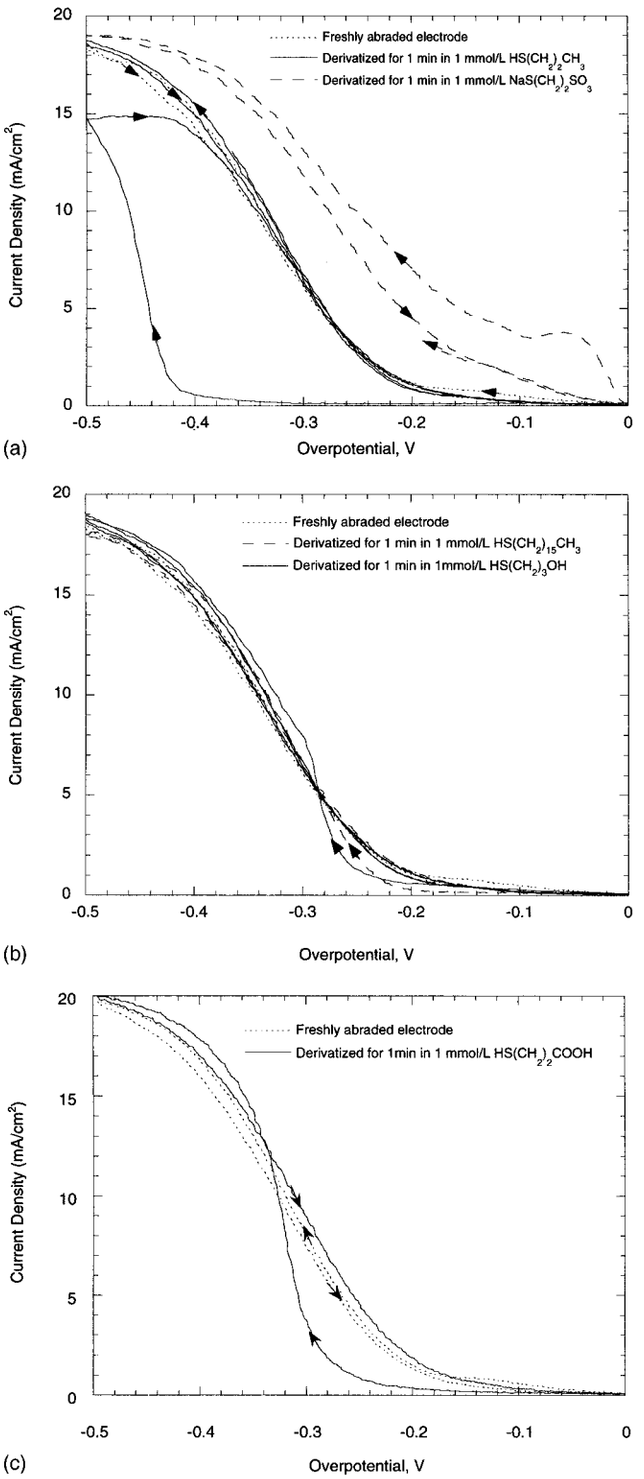

Figure 16. The η-i response for copper deposition on electrodes modified with different thiol molecules. Comparison with Fig. 9 demonstrates that catalytic activity is evident only for electrodes modified with thiols (or disulfides) having the SO_3^- terminal group. In contrast, derivatization with the other thiols initially results in greater hindrance to copper deposition than that provided by formation of the PEG-Cl^- blocking layer. This effect is evident only on the first negative-going sweep because the molecules are rapidly consumed and the electrode reverts to behavior characteristic of a freshly abraded electrode in the PEG-Cl electrolyte.

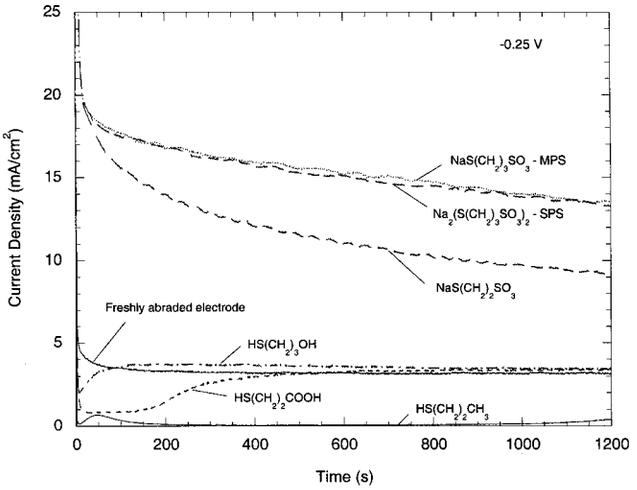

Figure 17. The key role of the catalyst terminal group is also evident in chronoamperometric studies. The electrodes were derivatized and then transferred for plating in a PEG-Cl electrolyte at -0.25 V. Of the molecules studied, only those with a sulfonate terminal group are capable of preventing formation of the passivating PEG-Cl^- film. Molecules with the hydrophilic -OH and reactive -COOH end groups are rapidly consumed during metal deposition, while the hydrophobic $-CH_3$ modified electrode exhibits significantly greater inhibition than that provided by PEG-Cl.

$-S(CH_2)_3OH$-modified electrode and $\sim$150 nm for the $-S(CH_2)_2COOH$-derivatized electrode. The $-S(CH_2)_2CH_3$-modified electrode exhibits significantly greater inhibition toward copper deposition which is sustained for several hundreds of seconds. The utility of combining the blocking attributes of $-S(CH_2)_2CH_3$ with the catalytic properties of the $-SO_3^-$ molecules for catalyzed through-mask plating, particularly using contact printing and/or related technologies, is a topic worthy of further attention.

These experiments unambiguously reveal the importance of the $-SO_3^-$ terminal group to the catalytic function of the accelerator. It is presumed that the charged end group disrupts the ability of PEG to form an effective rate-suppressing film on the surface of the copper electrode. The thiol, or disulfide, head group primarily tethers the $-SO_3^-$ end group to the surface. The charged end-group is also central to the molecules' ability to float, *i.e.*, segregate, on the growth surface during rapid ($\sim$30 ML/s) metal deposition. The importance of these heterogeneous interactions in superconformal film growth has been demonstrated in a related paper detailing bottom-up superfilling of trenches mediated by SPS-derivatized electrodes.[7]

Conventional wisdom associates brightening with grain refinement. On a more speculative front, the competitive adsorption model provides new avenues for thinking about the absence of crystalline anisotropy during film growth in the SPS-PEG-Cl system. If rate control for metal deposition resides with the tethered $-SO_3^-$ end group opening up prospective sites or channels in the blocking PEG layer, then the crystalline anisotropy evident during growth in additive-free systems might be further obscured. This would account for the smooth isotropic surfaces observed for metal films grown in the SPS-PRG-Cl system. It is also congruent with the success of the CEAC mechanism in describing shape evolution into the nanometer regime by simply tracking the local catalyst coverage.

A separate paper presents a quantitative description of the competitive adsorption dynamics between SPS and PEG-Cl and its influence on the copper deposition kinetics over a wide range of parameter space.[32]

Conclusions

The kinetics of copper electrodeposition from an acidified cupric sulfate electrolyte containing SPS-PEG-Cl were examined over a

wide range of parameters. Electroanalytical experiments reveal a competition between PEG and SPS for surface sites. PEG and Cl^- interact synergistically with Cu^+ to form a passivating film that can inhibit the metal deposition rate by two orders of magnitude. Subsequent adsorption of short chain disulfide or thiol molecules with sulfonate end group(s) leads to the disruption and/or displacement of the passivating surface complex and acceleration of the metal deposition rate, as evidenced by hysteretic voltammetry and rising chronoamperometric transients. Experiments with SPS-derivatized electrodes demonstrate that under conditions relevant to damascene processing, submonolayer quantities of catalyst remain segregated on the growth surface even after extensive metal deposition. The sulfonate end-group plays an important role in the surface segregation process. Multicycle voltammetry reveals a strong potential dependence for SPS adsorption as well as its subsequent deactivation. The rate of displacement of the blocking PEG layer by SPS adsorption increases with overpotential. Monitoring of the quenching of metal deposition rates on SPS-modified electrodes in a catalyst-free electrolyte permitted examination of catalyst deactivation, or consumption, without the complications of simultaneous catalyst accumulation. Catalyst consumption is a higher order process in catalyst coverage and exhibits a maximum rate near an overpotential of -0.1 V. Such derivatization experiments were found to be a particularly effective method for studying the role of molecular functionality in additive plating.

The National Institute of Standards and Technology assisted in meeting the publication costs of this article.

References

1. T. P. Moffat, D. Wheeler, W. H. Huber, and D. Josell, *Electrochem. Solid-State Lett.*, **4**, C26 (2001).
2. D. Josell, D. Wheeler, W. H. Huber, J. E. Bonevich, and T. P. Moffat, *J. Electrochem. Soc.*, **148**, C767 (2001).
3. D. Wheeler, D. Josell, and T. P. Moffat, *J. Electrochem. Soc.*, **150**, C302 (2003).
4. B. C. Baker, C. Witt, D. Wheeler, D. Josell, and T. P. Moffat, *Electrochem. Solid-State Lett.*, **6**, C67 (2003), and references therein.
5. D. Josell, S. Kim, D. Wheeler, T. P. Moffat, and S. G. Pyo, *J. Electrochem. Soc.*, **150**, C368 (2003).
6. G. McFadden, S. R. Coriell, T. P. Moffat, D. Josell, D. Wheeler, W. Schwarzacher, and J. Mallett, *J. Electrochem. Soc.*, **150**, C591 (2003).
7. T. P. Moffat, D. Wheeler, C. Witt, and D. Josell, *Electrochem. Solid-State Lett.*, **5**, C49 (2002).
8. T. P. Moffat, B. Baker, D. Wheeler, and D. Josell, *Electrochem. Solid-State Lett.*, **6**, C59 (2003).
9. M. R. H. Hill and G. T. Rogers, *J. Electroanal. Chem. Interfacial Electrochem.*, **86**, 179 (1978).
10. M. Yokoi, S. Konishi, and T. Hayashi, *Denki Kagaku oyobi Kogyo Butsuri Kagaku*, **52**, 218 (1984).
11. J. R. White, *J. Appl. Electrochem.*, **17**, 977 (1987).
12. D. Stoychev and C. Tsvetanov, *J. Appl. Electrochem.*, **26**, 741 (1996).
13. G. A. Hope and G. M. Brown, in *Electrode Processes*, A. Wieckowski and K. Itaya, Editors, PV 96-8, p. 215, The Electrochemical Society Proceedings Series, Pennington, NJ (1996).
14. J. J. Kelly and A. C. West, *J. Electrochem. Soc.*, **145**, 3472 (1998).
15. J. J. Kelly and A. C. West, *J. Electrochem. Soc.*, **145**, 3477 (1998).
16. M. Yokoi, S. Konishi, and T. Hayashi, *Denki Kagaku oyobi Kogyo Butsuri Kagaku*, **51**, 460 (1983).
17. Z. Nagy, J. P. Blaudeau, N. C. Hung, L. A. Curtiss, and D. J. Zurawski, *J. Electrochem. Soc.*, **147**, L87 (1995).
18. J. P. Healy, D. Pletcher, and M. Goodenough, *J. Electroanal. Chem.*, **338**, 155 (1992).
19. D. M. Soares, S. Wasle, K. Weil, and K. Doblhofer, *J. Electroanal. Chem.*, **532**, 353 (2002).
20. T. P. Moffat, J. E. Bonevich, W. H. Huber, A. Stanishevsky, D. R. Kelly, G. R. Stafford, and D. Josell, *J. Electrochem. Soc.*, **147**, 4524 (2000).
21. U. Bertocci, *Electrochim. Acta*, **11**, 1261 (1966).
22. A. Molodov, G. N. Markosyan, and V. V. Losev, *Electrochim. Acta*, **17**, 701 (1972).
23. M. Yokoi, S. Konishi, and T. Hayashi, *Denki Kagaku oyobi Kogyo Butsuri Kagaku*, **51**, 310 (1983).
24. E. Gileadi and V. Tsionsky, *J. Electrochem. Soc.*, **147**, 567 (2000).
25. A. Jardy, A. Legal Lasalle-Molin, M. Keddam, and H. Takenouti, *Electrochim. Acta*, **37**, 2195 (1992).
26. H. A. Biebuyck, C. D. Bain, and G. M. Whitesides, *Langmuir*, **10**, 1825 (1994).
27. Ch. Jung, O. Dannenberger, Y. Xu, M. Buck, and M. Grunze, *Langmuir*, **14**, 1103 (1998).
28. (a) S. M. Driver and D. P. Woodruff, *Surf. Sci.*, **488**, 207 (2001); (b) H. Kondoh, N. Saito, F. Matsui, T. Yokoyama, T. Ohta, and H. Kuroda, *J. Phys. Chem. B*, **105**, 12870 (2001); (c) M. J. Esplandiu, H. Hagenstrom, and D. M. Kolb, *Langmuir*, **17**, 828 (2001).
29. S. G. Malhotra, P. S. Locke, A. H. Simon, J. Fluegel, P. DeHaven, D. G. Hemmes, R. Jackson, and E. Patton, in *Advanced Metallization Conference 1999*, M. E. Gross, T. Gessner, N. Kobayashi, and Y. Yasuda, Editors, p. 77, MRS, Warrendale, PA (2000).
30. B. Baker, D. Pena, M. Herrick, R. Chowdhury, E. Acosta, C. R. Simpson, and G. Hamilton, in *Electrochemical Processing in ULSI Fabrication and Semiconductor/Metal Deposition II*, P. C. Andricacos, P. C. Searson, C. Reidsema-Simpson, P. Allongue, J. L. Stickney, and G. M. Oleszek, Editors, PV 99-9, p. 103, The Electrochemical Society Proceedings Series, Pennington, NJ (1999).
31. P. C. Andricacos, C. Parks, C. Cabral, R. Wachnik, R. Tsai, S. Malhtra, P. Locke, J. Fluegel, J. Horkans, K. Kwietniak, C. Uzoh, K. P. Rodbell, L. Gignac, E. Walton, D. Chung, and R. Geffken, in *Electrochemical Processing in ULSI Fabrication and Semiconductor/Metal Deposition II*, P. C. Andricacos, P. C. Searson, C. Reidsema-Simpson, P. Allongue, J. L. Stickney, and G. M. Oleszek, Editors, PV 99-9, p. 111, The Electrochemical Society Proceedings Series, Pennington, NJ (1999).
32. T. P. Moffat, D. Wheeler, M. Edelstein, and D. Josell, *IBM J. Res. Dev.*, Submitted.
33. H. Hagenstrom, M. A. Schneeweiss, and D. M. Kolb, *Langmuir*, **15**, 7802 (1999).
34. P. L. Schilardi, O. Azzaroni, and R. C. Salvarezza, *Phys. Rev. B*, **62**, 13098 (2000).
35. D. Roha and U. Landau, *J. Electrochem. Soc.*, **137**, 824 (1990).
36. J. Edwards, *Trans. Inst. Met. Finish.*, **41**, 169 (1964).
37. D. Stoychev, I. Vitanova, R. Bujukliev, N. Petkova, I. Popova, and I. Poljarliev, *J. Appl. Electrochem.* , **22**, 978 (1992).
38. D. Stoychev, I. Vitanova, R. Bujukliev, N. Petkova, I. Popova, and I. Poljarliev, *J. Appl. Electrochem.* , **22**, 987 (1992).
39. S. D. Evans, A. Ulman, K. E. Goppert-Berarducciand, and L. J. Gerenser, *J. Am. Chem. Soc.*, **113**, 5866 (1991); M. Brust, P. M. Blass, and A. J. Bard, *Langmuir*, **13**, 5602 (1997); T. Yamaguchi, R. Sakai, K. Takahashi, and T. Komura, *Electrochim. Acta*, **48**, 589 (2003).
40. E. D. Eliadis, R. G. Nuzzo, A. A. Gewirth, and R. C. Alkire, *J. Electrochem. Soc.*, **144**, 96 (1997).
41. H. Hagenstron, M. J. Esplandiu, and D. M. Kolb, *Langmuir*, **17**, 839 (2001).
42. O. Cavalleri, A. M. Bittner, H. Kind, K. Kern, and T. Greber, *Z. Phys. Chem. (Munich)*, **208**, 107 (1999).